Asian Herpetological Research 2016, 7(2): 112–121
DOI: 10.16373/j.cnki.ahr.150055

ORIGINAL ARTICLE

Comparison of Skull Morphology in Two Species of Genus *Liua* (Amphibia: Urodela: Hynobiidae), *L. shihi* and *L. tsinpaensis*

Jianli XIONG[1, 2*], Xiuying LIU[3] and Xiaomei ZHANG[3]

[1] *Animal Science and Technology College, Henan University of Science and Technology, Luoyang* 471003, *Henan, China*
[2] *Key Laboratory of Bio-resources and Eco-environment, Ministry of Education, School of Life Sciences, Sichuan University, Chengdu* 610064, *Sichuan, China*
[3] *School of Agriculture, Henan University of Science and Technology, Luoyang* 471003, *Henan, China*

Abstract Skull characteristics play an important role in the systematics of tailed salamanders. In this study, the skulls of *Liua shihi* and *L. tsinpaensis* were compared using a clearing and double-staining technique. The results showed that in *L. tsinpaensis*, the vomerine tooth rows are in a "⌒⌒" shape, the length of the inner vomerine tooth series is nearly equal to that of the outer series, the vomerine tooth rows do not extend beyond the choanae, an ossified articular bone is absent, the basibranchial is rod shaped, the radial loops exhibit a figure-eight shape, the cornua has two cylindrical branches, the urohyal is rod shaped, and the end of the ceratohyal is not ossified; these features differ considerably from those of *L. shihi*. The ossification of the posterior portion of the ceratohyal and the present or absent of ossified articular might represent ecological adaptation to feeding in different environments.

Keywords *Liua shihi*, *Liua tsinpaensis*, morphology, adaptation, systematics

1. Introduction

The genus *Liua* is an endemic genus of Chinese salamander that was proposed by Zhao and Hu (1983) based on the species *Ranodon wushanensis* (= *Hynobius shihi* Liu, 1950 = *Ranodon shihi* Risch and Thorn, 1981). However, the validity of the genus *Liua* was debated for many years (Xiong *et al.* (2012) for more details) until molecular data confirmed its legitimacy (Li *et al.*, 2004; Wang *et al.*, 2005; Zeng *et al.*, 2006; Zhang *et al.*, 2006; Zheng *et al.*, 2011; Xia *et al.*, 2012; Weisrock *et al.*, 2013). The validity of the genus is now widely accepted (AmphibiaWeb, 2015; Frost, 2015).

In addition to its type species, *L. shihi*, the genus *Liua* includes another species, *L. tsinpaensis* (Zeng *et al.*, 2006). The generic assignment of *L. tsinpaensis* has also been questioned for many years. *L. tsinpaensis* was first described as a new species of the genus *Ranodon* based on specimens from Hou-tseng-tze, Chouchih Hsien, and Shensi (Shanxi), China (Hu *et al.*, 1966). The characteristics used to justify this assignment included a lack of labial folds, vomerine teeth arranged in two curved rows, and an absence of cornification on the ventral surface of the feet (Hu *et al.*, 1966). Subsequently, Fei and Ye transferred *L. tsinpaensis* to the genus *Pseudohynobius* as *P. tsinpaensis* based on the characteristic shape, length, and location of the vomerine tooth rows as well as the shape of the skull and the labial folds (Fei and Ye, 1983). However, Zhao (1990) and Zhao and Wu (1995) suggested that *R. tsinpaensis* should be retained within the genus *Ranodon*. Based on molecular phylogenies, *L. tsinpaensis* clustered with *L. shihi* and not with *R. sibiricus* (the type species of *Ranodon*) or *P. flavomaculatus* (the type species of *Pseudohynobius*) (Zeng *et al.*, 2006). This clustering was confirmed by further molecular studies (Zhang *et al.*, 2006; Zheng *et al.*, 2011; Xia *et al.*, 2012; Weisrock *et al.*, 2013). Consequently, Zeng *et al.* (2006) transferred *L. tsinpaensis* into the genus *Liua*.

Skull morphology in particular has proven useful for systematics and phylogeny in Urodela (Wake, 1966;

* Corresponding author: Dr. Jianli XIONG, from Animal Science and Technology College, Henan University of Science and Technology, Luoyang, Henan, China, with his research mainly focusing on the systematics and evolution of amphibians and reptiles.
E-mail: xjlpanda@126.com
Received: 23 August 2015 Accepted: 15 March 2016

Duellman and Trueb, 1994; Ehmcke and Clemen, 2003). Zhao and Zhang (1985) cursorily described the skeleton of *L. tsinpaensis* and *L. shihi*, but this work is not sufficiently detailed to provide the basis for effective interspecific comparisons. In the present study, we systemically describe and compare the skull elements of *L. tsinpaensis* and *L. shihi*. Our aims were to present precise schematic drawings to illustrate details more clearly than in previous studies, and to draw attention to species-specific characteristics.

2. Materials and Methods

Seven adult specimens of *L. shihi* (4 males and 3 females) were collected from the type location, Wushan County, Chongqing Municipality, China (Figure 1). Four adult specimens of *L. tsinpaensis* (4 females) were collected from the type location, Zhouzhi County, Shanxi Province, China (Figure 1). Upon arrival at the laboratory, animals were euthanized via submergence in a buffered MS-222 solution. The anesthetized animals were prepared, fixed in 10% formalin, and then cleared and double-stained using a standard bone-cartilage staining procedure (Hanken and Wassersug, 1981). The specimens were skinned, and the eyes and viscera removed from the body cavity; the specimens then were washed in several changes of distilled water and placed in a solution of alcian blue 8GX for cartilage staining. For dehydration, the specimens were treated twice with absolute alcohol; re-hydrated through a graded, decreasing series of alcohol solutions; and then macerated twice in distilled water. For bone staining, the specimens were then placed in a solution of 0.5% KOH to which an alizarin red S stock solution had been added until the solution turned deep purple. Subsequently, the specimens were transferred to 100% glycerin via a graded series of glycerin 0.5% KOH solutions for clearing. Finally, the specimens were stored in fresh glycerin. The prepared skull was examined and photographed with a LEICA MZ6.0 binocular dissecting microscope (Leica Microsystems GmbH, Wetzlar Germany). Figures were drawn according to the method of Liu and Xiong (2013). Voucher specimens were deposited at the Museum of Sichuan University (SCUM).

For the nomenclature of skull morphology, we primarily adhered to the terminology of Jömann *et al.* (2005), which has also been adopted by Xiong *et al.* (2007, 2011a, 2011b, 2013) and Peng *et al.* (2010).

3. Results

The skulls of *L. shihi* and *L. tsinpaensis* consist of two components: cartilage and bone. Most of the skeletal elements are bone, and a few are cartilage. In *L. shihi*, the shape of the upper jaw describes a trapezium and

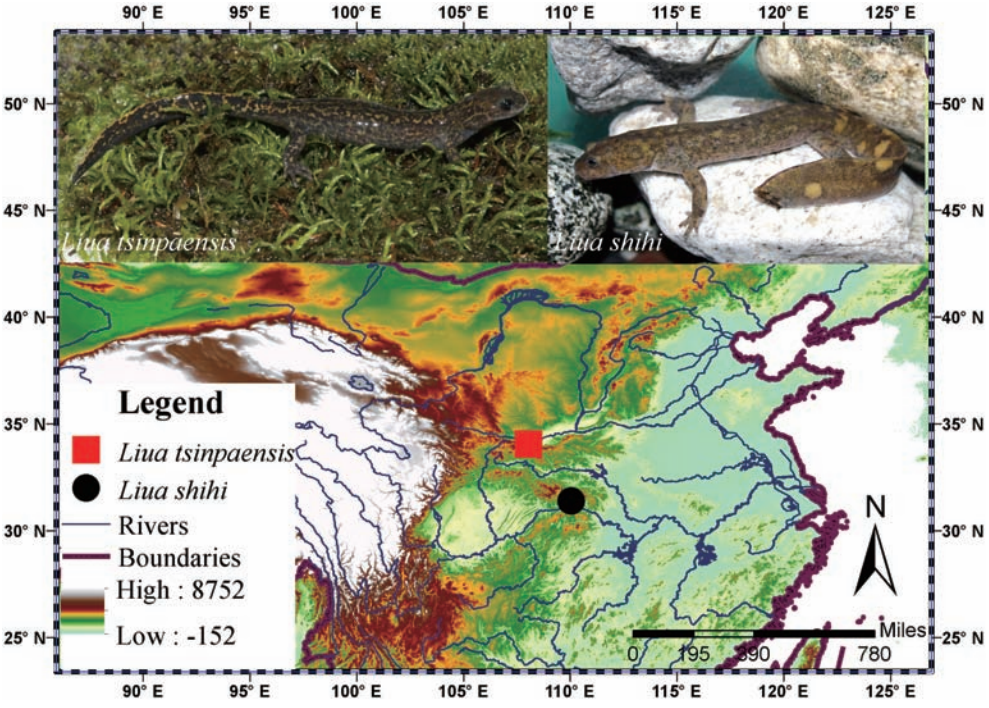

Figure 1 The localities of specimens used in this study. The collection site of *Liua shihi* is marked by a black circle; the collection site of *Liua tsinpaensis* is marked by a red square.

the space between the maxillaries is smaller than the space between the quadrates (Figure 2), whereas in *L. tsinpaensis*, the shape of the upper jaw describes a semi-circle and the space between the maxillaries is nearly equal to the space between the quadrates (Figure 3). The elements of the skulls of the two species are as follows (Figures 2 and 3).

Premaxilla: The paired premaxillae—articulated with each other at the most anterior point of the skull—have three distinct regions: the *pars dentalis*, the *pars palatina*, and the *processus dorsalis praemaxillaris* (also called the *pars frontalis*). The toothed *pars dentalis* forms the anterior border of the upper jaw and the ventral border of the external naris. The posterolateral edge of the *pars dentalis* articulates with the anterior tip of the *pars dentalis* of each maxilla. The joint is covered by the nasal cartilage in the dorsal view. The *pars palatina*—attached to the posterior margin of the *pars dentalis* and forming the anterior portion of the bony palate—is the posterior extension of the *pars dentalis*. The posterior edge of the *pars palatina* articulates with the anterior margin of the body of the vomer. The *processus dorsalis praemaxillaris*—ascending dorsally from the *pars dentalis*, parallel to the longitudinal axis of the skull, and forming the anterolateral border of each external naris—is deeply embedded in the nasal bone. The *processus dorsalis praemaxillaris* is longer and more attenuate in *L. shihi* and shorter and more robust in *L. tsinpaensis*.

Maxilla: The paired maxillae, together with the anteromedial premaxillae, form the upper jaw. Similar to the premaxillae, the maxilla is composed of three regions: the *pars dentalis*, the *pars palatina*, and the *processus facialis maxillaris*. The tooth-bearing *pars dentalis*, the primary component of the maxilla, articulates with the *pars dentalis* of the premaxilla anteriorly and extends posteriorly to form the arch of the upper jaw. The ventral surface of the *pars dentalis* bears numerous pedicellate teeth, except on the posterior portion. The length of the toothless portion of the *pars dentalis* is shorter in *L. tsinpaensis* than in *L. shihi*. The posterior end of the *pars dentalis* is more attenuate and reaches the middle of the orbit in *L. tsinpaensis*, whereas it is more robust and reaches one-third of the orbit in *L. shihi*. The posterior end of the *pars dentalis* is not sutured to the anterior end of the pterygoid and only connects with the pterygoid via cartilaginous tissue. The cartilaginous tissue is conjoint with the posterior end of the *pars dentalis* in *L. tsinpaensis* and not conjoint in *L. shihi*. The *pars palatina* is the extension of the *pars dentalis* into the oral cavity. This structure forms the anterolateral portions of the palate and the anterolateral border of the orbit. The *pars palatina* terminates near the toothless region of the *pars dentalis*. The *processus facialis maxillaris* arises from the anterior portion of the *pars dentalis* and extends dorsally, overlapping with the anterior portion of the lacrimal bone and the lateral portion of the prefrontal bone. The anterior margin of the *processus facialis maxillaris* forms the lateral border of the external naris; the posterior margin forms the anterodorsal border of the orbit.

Septomaxilla: The paired septomaxillae, embedded in the nasal cartilages of the nasal capsules at the lateral edge of the nasal vacuity, are small and irregular in shape. These structures are larger in *L. shihi* than in *L. tsinpaensis*.

Nasal: The paired nasals are bony plates that cover much of the dorsal surface of the cartilaginous nasal capsule. The anterolateral margin of the nasal bone forms the posterolateral edge of the external naris. The nasal bone articulates with the *processus dorsalis praemaxillaris* anteriorly, slightly overlapping the anterior portion of the frontal posteriorly. The premaxillary fontanelle is situated between the premaxillaries and nasals. The premaxillary fontanelle is larger in *L. tsinpaensis* than in *L. shihi*. The nasal articulates posterolaterally with the anterior portion of the prefrontal bone and the lacrimal bone in *L. tsinpaensis* but does not articulate with these two bones in *L. shihi* due to a gap.

Prefrontal: The paired prefrontal bones are located immediately anterior to the orbit and form its anterodorsal border. These bones are widely separated and do not contact each other at any point. The prefrontal is rectangular, slightly covered by the nasal bone anterolaterally and by the lacrimal bone anteriorly, and overlapped the anterolateral portion of the frontal posterolaterally in *L. tsinpaensis*. The prefrontal is a long strip covered by the lacrimal anteriorly and overlapped a greater portion of the frontal posterolaterally in *L. shihi*.

Frontal: The paired frontals, which are close to each other mesially without fusing, form the anterior roof of the braincase. The anterior portion is covered by the posterior edges of the nasal and prefrontal. Posteriorly, the attenuate end overlaps the anterior edge of the parietal. The lateral edge descends and articulates with the orbitosphenoid. The anterolateral portion forms the dorsal rim of the orbit. The frontal of *L. tsinpaensis* is more robust than it is in *L. shihi*, but the posterior end is more attenuate in *L. shihi* than it is in *L. tsinpaensis*.

Parietal: The paired parietals are close to each other and cover the posterior braincase. The anterior portion of the parietal underlies the posterior edge of the frontal anteriorly, overlaps the anteromedial portion of the

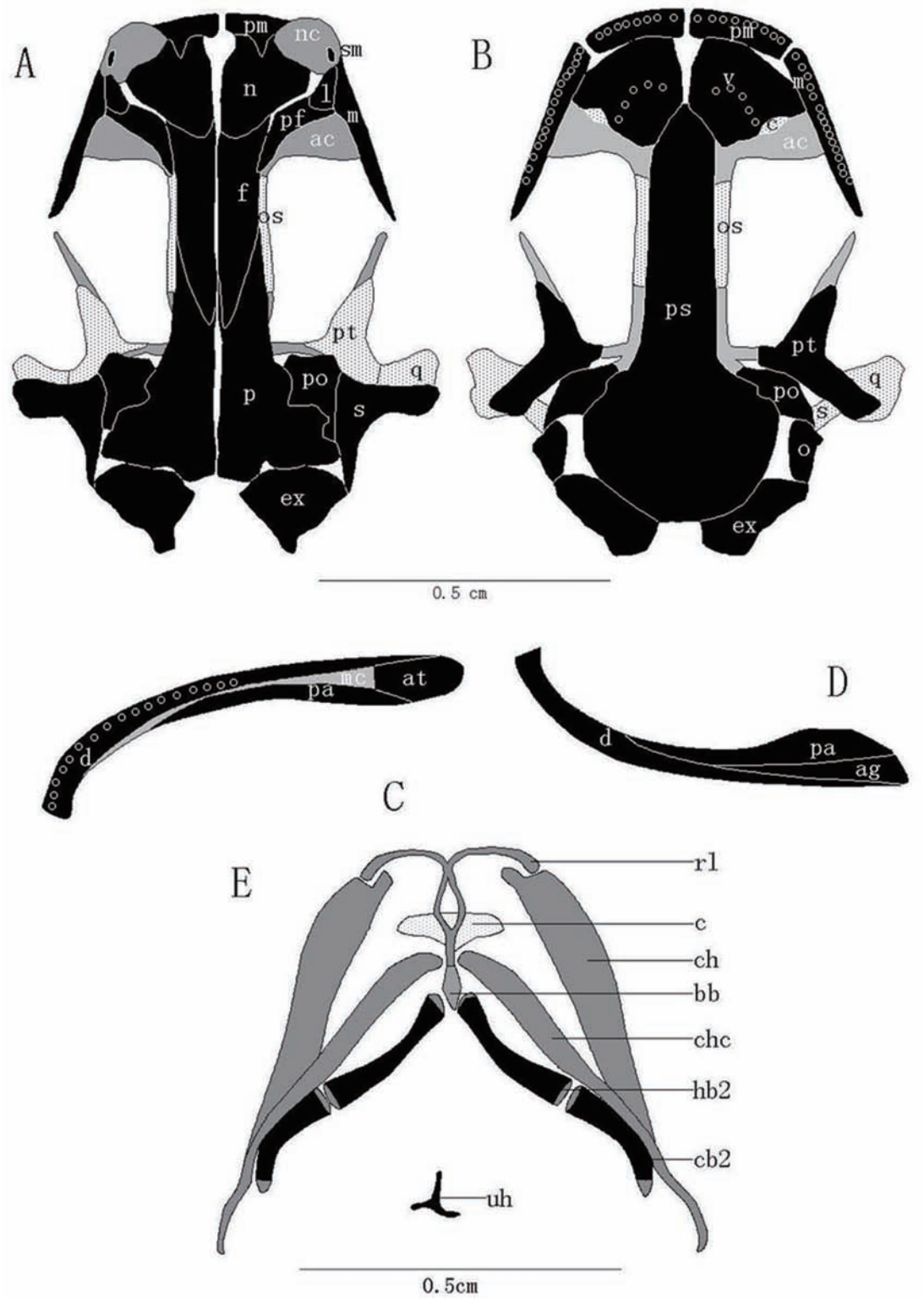

Figure 2 Diagrammatic drawing of skulls of *Liua shihi*. A: skull, dorsal view; B: skull, ventral view; C: lower jaw, dorsal view; D: lower jaw, ventral view; E: the hyobranchial apparatus. Bones are shown in black or white with black dots (in deeper zones of the skull); cartilage is shown in gray or white with gray dots (in deeper zones); teeth are represented by open circles; and gaps or foramina are shown in white. Abbreviations: ac–antorbital cartilage, ag–angular, at–articular, c–choana, d–dentary, ex–exoccipital, f–frontal, l–lacrimal, m–maxillary, mc–Meckel's cartilage, n–nasal, nc–nasal cartilage, o–operculum, os–orbitosphenoid, p–parietal, pa–prearticular, pf–prefrontal, pm–premaxilla, po–prootic, ps–parasphenoid, pt–pterygoid, q–quadrate, s–squamosal, sm–septomaxilla, v–vomer, bb–basibranchial, c–cornua, rl–radial loop, ch–ceratohyal, chc–complex of hypobranchial I and ceratobranchial I, hb2–hypobranchial II, cb2–ceratobranchial II, uh–urohyal. Figure 2E: Adapted from Xiong *et al.* (2013).

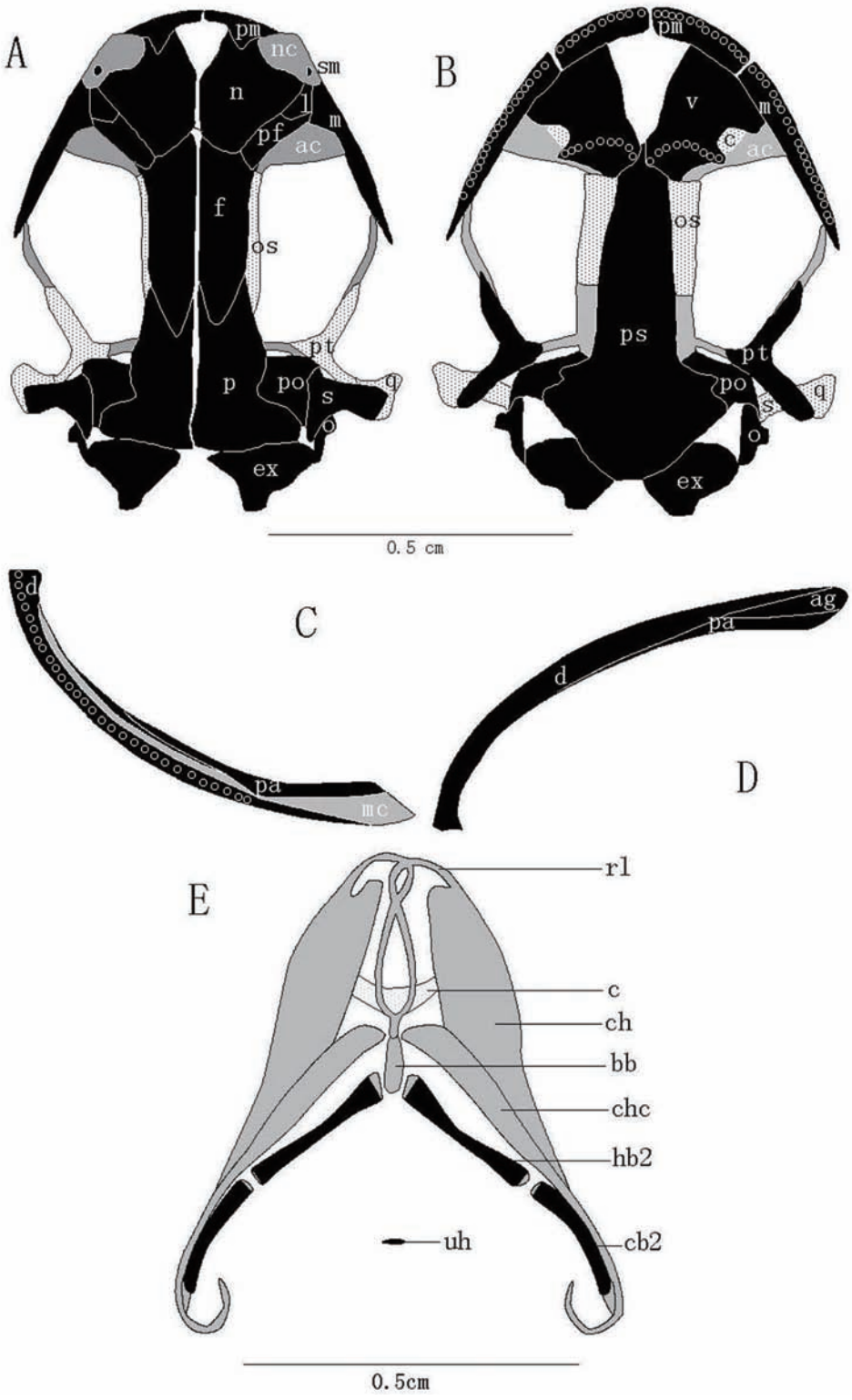

Figure 3 Diagrammatic drawing of the skull of *Liua tsinpaensis*. Abbreviations and coloring as in Figure 2.

exoccipital, articulates with the posterior part of the orbitosphenoid ventrally, and contacts the squamosal and prootic laterally. The posterior tip of the parietal reaches the caudal end of the skull. The parietal is longer in *L. shihi* than in *L. tsinpaensis*.

Lacrimal: The paired lacrimal bones—specific to hynobiid, rhyacotritonid, and dicamptodontid salamanders—are situated laterally to the prefrontals. The

anterior portion forms the rim of external naris, the lateral portion is covered by the *processus facialis maxillaries*, the posterolateral portion is overlapped the prefrontal, and the posterior portion does not extend to the orbit. The anterior portion of the lacrimal is overlapped by the nasal in *L. tsinpaensis* but not overlapped by the nasal in *L. shihi*.

Squamosal: The paired squamosals extend from the otic capsules to the quadrates and are fixed to the lateral area of the upper skull. This structure has three processes. The anterior process articulates with the prootic, the posterior process articulates with the lateral portion of the parietal and the operculum, and the ventral process—the largest process—overlaps the quadrate and the posterior portion of the pterygoid. The squamosal is less developed in *L. tsinpaensis* than in *L. shihi*.

Prootic: The paired prootics are the primary component of the otic capsule. In the dorsal view, they articulate with the parietal and the squamosal and slightly overlaps the pterygoid anteriorly. In the ventral view, they articulate with the parasphenoid and the pterygoid.

Exoccipital: The paired exoccipitals enclose the foramen magnum and form the posteromedial walls of the otic capsule. In the dorsal view, the exoccipital articulates with the posterior portion of the parietal anteriorly and with the operculum laterally. There is a space among the parietal, the exoccipital, the operculum, and the squamosal that accommodates the posterior process of the squamosal. In the ventral view, the exoccipital articulates with the posterior portion of the parasphenoid and the operculum. Similar to the dorsal view, there is a space among the parasphenoid, the exoccipital, the operculum, and the prootic. The posterior portion of the exoccipital, called the occipital condyle, arises as a cylindrical, bony extension lateroventral to the *foramen magnum*. The occipital condyle and the odontoid facet, on the lateral wall of the *foramen magnum*, articulate with the condylar facet and odontoid process of the atlas, respectively.

Operculum: The operculum is located along the posterolateral surface of the squamosal, and together with the exoccipital and prootic, forms the otic capsule. The external surfaces of the operculum are slightly convex, and a distinct columella is fused with the operculum. The operculum articulates with the exoccipital posteriorly and with the squamosal anteriorly. The distal end of operculum is attached by a cartilaginous piece to the pterygoquadrate cartilage. In *L. shihi*, the operculum cannot be seen in the dorsal view because it is covered by the squamosal.

Vomer: The paired vomers form the dorsal and anterior roof of the oral cavity as well as the posterior floor of the nasal capsule. The anterior portion is a broad, toothless, and dorsally convex plate that contacts with the *pars palatina* of the premaxilla anteriorly and the maxilla anterolaterally. There is a wide gap between the vomers, which is the site of a glandular complex that extends from the roof of the oral cavity to the dorsal surface of the head, between the frontal processes of premaxillae. This gap is larger in *L. tsinpaensis* than it is in *L. shihi*.

The posterolateral portion of the vomer forms the medial rim of the internal naris. The posterior portion of the vomer overlaps the anterior portion of the parasphenoid. The middle and posterior portions of the vomer bear small teeth on the medial edge, called vomerine teeth, which occur in rows. In *L. shihi*, there are only a few teeth (ranging from 4 to 7) and the vomerine tooth rows are not connected at the midline, thus forming a "⌒" shape. The tooth rows can be distinguished as an inner and an outer series. The outer series is longer than the inner series. The inner series begins at the middle of the vomer, and the outer series ends at the posterior choanae. The anterior portion of the tooth rows extends beyond the anterior edge of the internal nare. In *L. tsinpaensis*, there are more teeth (ranging from 6 to 9) than in *L. shihi* and the vomerine tooth rows are not connected at the midline, thus forming a "⌒⌒" shape. The tooth rows can also be distinguished as an inner and an outer series; the inner series, however, is nearly equal to the outer series. The inner series begins at the end of the vomer, and the outer series ends at the posterior internal nare; the anterior portion of the tooth rows does not extend beyond the anterior edge of the internal naris.

Orbitosphenoid: The vertically oriented orbitosphenoid is an endochondral ossification that forms the lateral portion of the braincase. Its shape is nearly rectangular. The orbitosphenoid articulates dorsally with the ventral surface of the frontal, parietal, and prefrontal and articulates with the vomer and parasphenoid ventrally.

Quadrate: The quadrate, a blocky bone, is part of the suspensory apparatus of the mandible. The quadrate is overlain dorsally by the squamosal, covers the pterygoid dorsolaterally, and articulates with the prootic laterally. The lateral surface accommodates an articular surface between the quadrate and the articular.

Parasphenoid: The single, sword-shaped parasphenoid is the largest bone in the skull. This bone forms the posterior roof of the oral cavity and the floor of the braincase. It also provides support for the posterior portion of the nasal capsule and overlaps the otic capsule posteriorly. The posterior end of the parasphenoid reaches

the *foramen magnum*. The parasphenoid articulates with the orbitosphenoid dorsally, with the vomers anteriorly, with the prootic laterally, and with the exoccipital posterolaterally. The anterior half is slightly narrower than the posterior half. The widest portion of the parasphenoid is situated slightly behind the prootic.

Pterygoid: The L-shaped pterygoid is another part of the suspensory apparatus of the mandible and has three obvious processes (anterior, lateral, and posterolateral). The anterior process extends toward the maxilla. The lateral process is the shortest of the three processes. The posterolateral process is the longest and most stout process. The pterygoid forms the ventral border of the orbit and articulates with the inner side of the quadrate and the anterior wall of the prootic posteriorly. The pterygoquadrate cartilage is involved as well in pterygoid.

Dentary: The dentary is the major bone of the mandibular ramus. Its anterior portion, approximately three-quarters of the length of the dentary, bears teeth. The posterior portion of the dentary resembles a vertically oriented, thin blade and gradually becomes attenuate.

Meckel's cartilage: Meckel's cartilage is enclosed by the dentary and the prearticular, and the anterior end nearly reaches the anterior end of the dentary. The posterior end is ossified to the articular in *L. shihi*, whereas it is not ossified in *L. tsinpaensis*.

Prearticular: The prearticular inserts on the lingual side of the dentary, forming the lingual border of the posterior half of the ramus. A coronoid process arises on its dorsal surface and inflects lingually.

Articular: The articular, lies between dentary and prearticular and originates from the ossification of the posterior part of Meckel's cartilage, articulates with the quadrate of the skull to form the mandibular joint. In *L. shihi*, the ossified articular is present in six specimens (the degree of ossification is same as shown in Figure 2) and absent in one smallest specimen. In *L. tsinpaensis*, the ossified articular is absent in all examined specimens.

Angular: The angular is located at the posteroventral side of the mandibular ramus and forms the posterior portion of the mandibular ramus. The angular is longer in *L. shihi* than it is in *L. tsinpaensis*.

Basibranchial: The basibranchial is located in the midline of the hyobranchial apparatus, which is a cartilaginous element and articulates with the paired hypobranchials. The central portion of the basibranchial bears a tubercle. The ends of the paired radial loops are fused and articulate with the basibranchial via the tubercle. The basibranchial is rhombic in shape in *L. shihi* and rod-shaped in *L. tsinpaensis*.

Cornua: The cornua is a cartilage situated under the radial loop. The cornua is fan shaped in *L. shihi*, whereas it has two cylindrical branches gradually tapering anterolaterally to a pointed tip in *L. tsinpaensis*.

Radial loop: The paired radial loops lie in the anterior portion of the basibranchial; these loops cross in a figure-eight fashion over the midline and connect the two ceratohyals in *L. tsinpaensis*, and they cross in an "o" shape in *L. shihi*. The tip of the radial loop articulates with the ceratohyal in *L. shihi* and fuses with the ceratohyal in *L. tsinpaensis*.

Ceratohyal: The paired ceratohyals are broad, flat cartilages that lie lateral and anterior to the other parts of the hyobranchial apparatus. The anterior portion of each forms a flattened blade, and the posterior portion is cylindrical. The ceratohyals are partially ossified in *L. shihi* but are not ossified in *L. tsinpaensis*.

Complex of the hypobranchial I and the ceratobranchial I: The complex of the hypobranchial I and the ceratobranchial I is composed of cartilage. The anterior ends of the complex are broad and become gradually attenuated posteriorly. The ends of the complex extend over the ends of the ceratohyal and the ceratobranchial II and gradually taper posterolaterally, forming curved ends in *L. tsinpaensis* and an undulating shape in *L. shihi*.

Hypobranchial II: The paired hypobranchial II are ossified, slightly sigmoidal and cylindrical, and longer than the ceratobranchial II. The hypobranchial II appears more robust in *L. shihi* than in *L. tsinpaensis*.

Ceratobranchial II: The posterior ends of the ceratobranchial II are not completely ossified. The posterior end of the ceratobranchial II and the complex of the hypobranchial I and ceratobranchial I overlap the posterior end of the ceratohyal in *L. tsinpaensis*, but they do not do so in *L. shihi*. Similar to the hypobranchial II, the ceratobranchial II is more robust in *L. shihi* than it is in *L. tsinpaensis*.

Urohyal: The single urohyal lies medially, slightly posterior to the level of the ends of the ceratobranchial II. The urohyal is present as a small rod of ossified tissue in *L. tsinpaensis* and has a decidedly tri-radiate shape in *L. shihi*.

4. Discussion

The skulls of *L. shihi* and *L. tsinpaensis* are generally similar in structure; however, some obvious differences can be detected (i.e., the shape of vomerine tooth row, the relative lengths of the inner and outer series, the

spatial relationship between the vomerine tooth rows and the choanae, ossified articular, and the shape of the basibranchial, the radial loops, the urohyal, the cornua, and the upper jaw) (Table 1).

In the systematics of the hynobiid salamanders, vomerine teeth (including the shape of the vomerine tooth rows, as well as the spatial relationship between the vomerine tooth rows and the choanae) are important, especially in the diagnoses of genera (Liu, 1950; Zhao and Hu, 1984; Zhao and Adler, 1993; Fei *et al.*, 2006). In this respect, *L. tsinpaensis* differs from *L. shihi* (Table 1). First, the vomerine teeth of *L. tsinpaensis* are arranged in a "⌒⌒" shape, and the inner series is nearly equal in length to the outer series, whereas those of *L. shihi* are arranged in a "⌒" shape, and the outer series is obviously longer than the inner series. Second, the vomerine tooth rows of *L. tsinpaensis* do not extend beyond the choanae and the inner series begins at the end of vomer, whereas the vomerine tooth rows of *L. shihi* extend beyond the choanae and the inner series begins at the middle of the vomer.

The morphology of the adult hyobranchial apparatus has played an important role in studies on the systematics of urodeles. For example, Wake (1963) used the absence or presence of the anterior process of the first basibranchial (basibranchial in the present study) and the relative length of the second basibranchial (urohyal in the present study) to diagnose the genera *Aneides*, *Plethodon*, and *Ensatina*. Moreover, Wake (1966) used the following characters to diagnose the subfamilies Desmognathinae and Plethodontinae: absence or presence of the anterior first basibranchial expansion; the first ceratobranchials (hypobranchials in the present study) or the epibranchials (ceratobranchial in the present study) as the longest of the articulated hyobranchial elements; the length of the first and second ceratobranchials; the relative lengths of the epibranchials and the first basibranchials, the epibranchials and the first ceratobranchials, and the second ceratobranchials and the first basibranchials; and the absence or presence of the second basibranchials (urohyal in the present study). Xiong *et al.* (2013) compared the hyobranchial apparatus of eight hynobiid species (representative of eight genera of Hynobiidae) and noted that the following differences could be used as diagnostic characters for species or genera: the basibranchial of *O. zhangyapingi* is ossified; the posterior ends of the ceratohyals are ossified in *B. pinchonii*, *P. shangchengensis*, and *L. shihi*; the hypobranchial I and ceratobranchial I are present as separate elements in *O. zhangyapingi*, *P. shangchengensis*, and *R. sibiricus*; the hypobranchial I of *P. shangchengensis* is ossified; and the urohyal is absent in *O. zhangyapingi*. In the present study, the characteristics of the hyobranchial apparatus in *L. tsinpaensis* (a rod-shaped basibranchial, a figure-eight radial loop, a rod-shaped urohyal, a cornua with two cylindrical branches, and the end of the ceratohyal not ossified) are different from those of *L. shihi* (Table 1). These differences reflect species-specific differences and could be used as diagnostic characters for species.

The habitats of *L. tsinpaensis* and *L. shihi* are considerably different. *L. tsinpaensis* is terrestrial and occurs in streams only during the breeding season, whereas *L. shihi* is aquatic for its entire life. Habitats drive morphological diversity among salamanders (Buckley *et al.*, 2010) because morphological specializations are the result of natural selection on morphology in response to specific functional or ecological demands (Herrel *et al.*, 2009). For example, the habitat of organisms determines their available prey items and exerts a strong influence on their feeding behavior (Özeti and Wake, 1969). The aquatic salamanders capture prey by rapidly expanding the mouth and throat, capturing prey by suction, whereas the terrestrial salamanders project a sticky tongue from the mouth to snare prey (Deban and Wake, 2000). The

Table 1 Comparison of major differences in skull characters between *Liua tsinpaensis* and *Liua shihi*.

Character	*Liua tsinpaensis*	*Liua shihi*
Shape of vomerine tooth row	⌒⌒	⌒
Length of inner and outer series	Equal	Outer longer than inner series
Spatial relationship between vomerine tooth rows and choanae	Not extending beyond the choanae	Extend beyond the choanae
Articular	Not present	Present
Shape of basibranchial	Rod-shaped	Rhombic
Shape of radial loops	Figure-eight shaped	O-shaped
End of ceratohyal	Not ossified	Partially ossified
Shape of cornua	Two cylindrical branches	Fan-shaped
Shape of urohyal	Rod-shaped	Tri-radiate shape
Shape of upper jaw	Semi-circle	Trapezoid

cranial architecture of salamanders is diverse and reflects adaptations to a variety of terrestrial and aquatic habitats (Duellman and Trueb, 1994). The posterior portion of the ceratohyal is ossified in *L. shihi* but not in *L. tsinpaensis*. The phenomenon of an ossified posterior portion of the ceratohyal is also found in other aquatic salamanders (Deban and Wake, 2000). The hyobranchial apparatus is the central component of the salamander feeding system (Deban, 2003). The cartilaginous ceratohyal may reduce the constraints limiting tongue protraction in terrestrial salamanders, and the ossified ceratohyal may increase the suction that can be generated in aquatic salamanders (Xiong *et al*., 2013). In these instances, a difference in the ossification of the posterior portion of the ceratohyal would represent an ecological adaptation. In a similar fashion, the greater degree of ossification of the articular may also represent an ecological adaptation. The articular is the expanded posterior portion of Meckel's cartilage (Francis, 1934) and the fact that it is so heavily ossified (typically not ossified in other salamanders, Duellman and Trueb, 1994) suggests an ecological role in these largely aquatic salamanders. The situation in *L. tsinpaensis* represents the ancestral, default state and thus it cannot be associated with a particular adaptation. However, the ossified bone in *L. shihi* doubtless contributes strength to the lower jaw and entire feeding system, likely improving feeding function in the more resistant aquatic medium in which feeding takes place.

Acknowledgements We are grateful to Guanfu Wu, Hui Zhao, and Xiaowu Xue of the Chengdu Institute of Biology (CIB), Chinese Academy of Sciences for the field help, and Pipeng Li of Institute of Herpetology and Liaoning Key Lab of Evolution and Biodiversity, Shenyang Normal University and Jun Yang of Sichuan University for providing part specimens. This work was supported by grants from the National Natural Science Foundation of China (NSFC 30900138, 31471971).

References

AmphibiaWeb. 2015. AmphibiaWeb: Information on amphibian biology and conservation. Berkeley, California: AmphibiaWeb. 2015. Available: http://amphibiaweb.org/ (Accessed: 10 Feb 2015)

Buckley D., Wake M. H., Wake, D. B. 2010. Comparative Skull Osteology of *Karsenia koreana* (Amphibia, Caudata, Plethodontidae). J Morphol, 271: 533–558

Deban S. M., Wake D. B. 2000. Aquatic feeding in salamanders. In Schwenk K. (Ed.), Feeding: Form, Function, and Evolution in Tetrapod Vertebrates. San Diego: Academic Press (65–94)

Deban S. M. 2003. Constraint and convergence in the evolution of salamander feeding. In Gasc J. P., Casinos A., Bels V. L. (Eds), Vertebrate Biomechanics and Evolution. Oxford: BIOS Scientific Publishers (163–180)

Duellman W. E., Trueb L. 1994. Biology of Amphibians. Baltimore and London: The Johns Hopkins Univeristy Press

Ehmcke J., Clemen G. 2003. The skull structure of six specis of Mesoamerican plethodontid salamanders (Amphibia, Urodela). Ann Anat, 185: 253–261

Fei L., Ye C. Y. 1983. Systematic studies on Hynobiidae, including diagnosis of a new genus *Pseudohynobius* (Amphibia: Caudata). Acta Herpetol Sin, 2: 31–37 (In Chinese)

Fei L., Hu S. Q., Ye C. Y., Huang Y. Z. 2006. Fauna Sinica: Amphibia, Vol. 1. Beijing: Science Press (In Chinese)

Francis E. T. B. 1934. The anatomy of the salamander. Oxford, UK: Clarendon Press

Frost D. R. 2015. Amphibian Species of the World: An online reference. Version 6.0. American Museum of Natural History, New York, USA. 2015. Available: http://research.amnh.org/herpetology/amphibia/index.html (Accessed: 20 Aug 2015)

Hanken J., Wassersug R. 1981. The visible skeleton. A new double-stain technique reveals the native of the "hard" tissues. Functional Photography, 16: 22–26

Herrel A., Deban S. M., Schaerlaeken V., Timmermans J. P., Adriaens, D. 2009. Are morphological specializations of the hyolingual system in chameleons and salamanders tuned to demands on performance? Physiol Biochem Zool, 82: 29–39

Hu S. Q., Zhao E. M., Liu C. C. 1966. A herpetological survey of the tsinling and Ta-Pa shan region. Acta Zool Sin, 18: 57–90 (In Chinese)

Jömann N., Clemen G., Greven H. 2005. Notes on cranial ontogeny and delayed metamorphosis in the hynobiid salamander *Ranodon sibiricus* Kessler, 1866 (Urodela). Ann Anat, 187: 305–321

Li Y., Wu M., Wang X. L. 2004. Phylogenetic relationship of Hynobiidae base on sequences of mitochondrial 16S ribosomal RNA gene. Acta Zool Sin, 50: 464–469 (In Chinese)

Liu C. C. 1950. Amphibians of western China. Fieldiana: Zoology Memoirs, Vol. 2, 117–176

Liu X. Y., Xiong J. L. 2013. A method of drawing biological black line chart using the ViewGIS software. Chin J Zool, 48: 200–205 (In Chinese)

Özeti N., Wake D. B. 1969. The morphology and evolution of the tongue and associated structures in salamamders and newts (family Salamandridae). Copeia, 1969: 91–123

Peng R., Zhang P., Xiong J. L., Gu H. J., Zeng X. M., Zou F. D. 2010. Rediscovery of *Protohynobius puxiongensis* (Caudata: Hynobiidae) and its phylogenetic position based on complete mitochondrial genomes. Mol Phylogenet Evol, 56: 252–258

Wake D. B. 1963. Comparative osteology of the plethodontid salamander genus *Aneides*. J Morphol, 113: 77–118

Wake D. B. 1966. Comparative osteology and evolution of the lungless salamanders, family Plethodontidae. Mem South Cal Acad Sci, 4: 1–111

Wang Y. H., Wang X. L., Fang S. G., Wu M. 2005. DNA fingerprinting analysis of some species of Hynobiidae genera and a discuss of their classification. J Zhejiang Univ (Nat Sci), 32: 79–82 (In Chinese)

Weisrock D. W., Macey J. R., Matsui M., Mulcahy D. G.,

Papenfuss T. J. 2013. Molecular phylogenetic reconstruction of the endemic Asian salamander family Hynobiidae (Amphibia, Caudata). Zootaxa, 3626(1): 77–93

Xia Y., Gu H. F., Peng R., Chen Q., Zheng Y. C., Murphy R., Zeng X. M. 2012. COI is better than 16S rRNA for DNA barcoding Asiatic salamanders (Amphibia: Caudata: Hynobiidae). Mol Ecol Res, 12: 48–56

Xiong J. L., Chen Q., Zeng X. M., Zhao E. M., Qing L. Y. 2007. Karyotypic, morphological, and molecular evidence for *Hynobius yunanicus* as a synonym of *Pachyhynobius shangchengensis* (Urodela: Hynobiidae). J Herpetol, 41(4): 664–671

Xiong J. L., Chen Y. Y., Zeng X. M. 2012. Catalogue of the Type Specimens of Amphibians and Reptiles in the Herpetological Museum of the Chengdu Institute of Biology, Chinese Academy of Sciences: II. Hynobiidae (Amphibia, Urodela). Asian Herpetol Res, 3(4): 327–333

Xiong J. L., Gu H. J., Gong T. J., Zeng X. M. 2011a. Redescription of an enigmatic salamander, Pseudohynobius puxiongensis (Fei et Ye, 2000) (Urodela: Hynobiidae). Zootaxa, 2919: 51–59

Xiong J. L., Liu X. Y., Zeng X. M. 2011b. Discovery of an Internasal Bone in Hynobius maoershanensis (Urodela: Hynobiidae). Asian Herpetol Res, 2(2): 87–90

Xiong J. L., Sun P., Zhang J. L., Liu X. Y. 2013. A comparative study of the hyobranchial apparatus in Hynobiidae (Amphibia: Urodela). Zoology, 116: 99–105

Zeng X. M., Fu J., Chen L. Q., Tian Y. Z., Chen X. H. 2006. Cryptic species and systematics of the hynobiid salamanders of the *Liua* - *Pseudohynobius* complex: Molecular and phylogenetic perspectives. Biochem Syst Ecol, 34: 467–477

Zhang P., Chen Y. Q., Zhou H., Liu Y. F., Wang X. L., Papenfuss T. J., Wake D. B., Qu L. H. 2006. Phylogeny, evolution, and biogeography of Asiatic salamanders (Hynobiidae). Proc Nat Acad Sci, 103: 7360–7365

Zhao E. M., Adler K. 1993. Herpetology of China. Oxford: Society for the Study of Amphibians and Reptiles

Zhao E. M., Hu Q. X. 1983. Taxonomy and evolution of Hynobiidae in Western China, with description of a new genus. Acta Herpetol Sin, 2(2): 29–35 (In Chinese)

Zhao E. M., Hu Q. X. 1984. Studies on Chinese tailed Amphibians. Chengdu: Sichuan Scientific and Technical Publishing House

Zhao E. M., Wu G. F. 1995. Taxonomic status of *Ranodon tsinpaensis* Liu and Hu, 1966, with a discussion on *Pseudohynobius flavomaculatus* (Fei and Ye, 1982) as its synonym. Sichuan J Zool, 14(1): 20–24 (In Chinese)

Zhao E. M., Zhang F. J. 1985. Comparative studies on the skeletons of *Ranodon*, *Batrachuperus*, *Liua* and *Xenobius* and their phylogeny. Acta Herpetol Sin, 4: 209–218

Zhao E. M. 1990. Notes on some taxonomic problems in Chinese salamanders with a revised list. In Zhao E. M. (Ed.), From Water onto Land. Beijing: China Forestry Publishing House (217–219)

Zheng Y. C., Peng R., Kuro-o M., Zeng X. M. 2011. Exploring patterns and extent of bias in estimating divergence time from mitochondrial DNA sequence data in a particular lineage: A case study of salamanders (Order Caudata). Mol Biol Evol, 28(9): 2521–2535